International Journal of Solids and Structures 48 (2011) 1754–1766

Contents lists available at ScienceDirect

International Journal of Solids and Structures

journal homepage: www.elsevier.com/locate/ijsolstr

Thickness effects in polycrystalline thin films: Surface constraint versus interior constraint

Haidong Fan, Zhenhuan Li *, Minsheng Huang, Xiong Zhang

Department of Mechanics, Huazhong University of Science and Technology, Wuhan 430074, China
Hubei Key Laboratory of Engineering Structural Analysis and Safety Assessment, Luoyu Road 1037, Wuhan 430074, China

ARTICLE INFO

Article history:
Received 7 September 2010
Received in revised form 29 January 2011
Available online 2 March 2011

Keywords:
Thickness effects
Polycrystalline thin films
Discrete dislocation dynamics
Surface passivation layers
Surface grain refinement

ABSTRACT

The uniaxial tension behavior of polycrystalline thin films, in which all grain boundaries (GBs) are penetrable by dislocations, is investigated by two-dimensional discrete dislocation dynamics (DDD) method with a penetrable dislocation-GB interaction model. In order to study thickness effect on the tensile strength of thin films with and without surface treatment, three types of thin films are comparatively considered, including the thin films without surface treatment, with surface passivation layers (SPLs) of nanometer thickness and with surface grain refinement zones (SGRZs) consisting of nano-sized grains. Our results show that thickness effects and their underlying dislocation mechanisms are quite distinct among different types of thin films. The thicker thin films without surface treatment are stronger than the thinner ones; however, opposite thickness effects are captured in the thin films with SPLs or SGRZs. Moreover, the underlying dislocation mechanisms of the same thickness effects of thin films with SPLs and SGRZs are different. In the thin films with SPLs, the thickness effect is caused by the sharp increase of dislocation density near the film-passivation interface, while it is mainly due to the sharp decrease of dislocation density within the refined surface grains of the thin films with SGRZs. No matter in what type of thin films, thickness effect gradually disappears when the number of grains in the thickness direction is large enough. Our analysis reveals that general mechanism of those thickness effects lies in the competition between the exterior surface-constraint and interior GB-constraint on gliding dislocations.

1. Introduction

With the startlingly rapid development of micro-technology, especially in micro-forming and micro-manufacturing, the ever-continuing miniaturization of various components/devices becomes an unstoppable trend. Once the leading sizes of the micro-components/devices decrease to the same order as the intrinsic lengths of materials, size effects appear and the mechanical behavior of small-sized materials remarkably deviates from that of bulk counterparts. Generally speaking, the intrinsic lengths of materials are usually at the micron or submicron scale (Arzt, 1998). For this reason, various thin films with micron/nanometer thicknesses, which are widely used in many micro-electronic and micro-electro-mechanical systems, commonly display strong size effects. A thorough understanding of the size dependent plasticity in thin films and its inherent mechanism is not only of academic significance, but also of great urgency to the reliability design and security assessment of various micro-electric and micro-electro-mechanical systems.

Recently, the micro-plasticity of thin films becomes an active research field (Keller et al., in press; Lee et al., 2011; Liang et al., 2009; Nicola et al., 2005b, 2006; Xiang et al., 2006; Xiang and Vlassak, 2006) due to the increasing application of thin films in micro-electric and micro-electro-mechanical systems. Different from single crystalline thin films, there are usually several grains in the thickness direction of polycrystalline thin films (Espinosa et al., 2006, 2004). At least two characteristic lengths (i.e., grain size and film thickness) strongly influence the tensile strength of polycrystalline thin films. The effect of grain size is associated with the interior grain boundary (GB)-constraint on dislocations (i.e., Hall–Petch effect); however, the thickness effect is mainly because of the weak exterior surface-constraint on dislocations. Both "GB engineering" method, i.e., manipulating GB structures or strengthening GBs in polycrystalline metals, and "surface engineering" method, i.e., refining surface grains or passivating surfaces of thin films can obtain the desired high strength. Obviously, the former method enhances the strengths of polycrystalline thin films by strengthening their interior constraint; however, the latter stiffens thin films by strengthening their exterior constraint. In recent years, these two methods have been broadly used to increase the strength of polycrystalline thin films (Geers et al., 2006; Nicola et al., 2006; Xiang and Vlassak, 2006).

* Corresponding author at: Department of Mechanics, Huazhong University of Science and Technology, Wuhan 430074, China. Fax: +86 27 87543501.
E-mail address: zhli68@263.net (Z. Li).

0020-7683/$ - see front matter © 2011 Published by Elsevier Ltd.
doi:10.1016/j.ijsolstr.2011.02.026

In order to understand the size effect on the tensile strength of polycrystalline thin films, massive efforts have been made in the past two decades but some deep-seated questions still remain open. For example, the polycrystalline thin films without surface treatment usually display strong thickness effect when subjected to pure tensile loading: thicker is stronger (Keller et al., in press; Miyazaki et al., 1979; Raulea et al., 2001; Tsai et al., 2005). This thickness effect is believed to be closely associated with the relatively easy deformation of surface grains owing to the weak exterior free surface-constraint. On the other hand, when thin films are passivated with SPLs, the opposite thickness effect is observed: thinner is stronger (Nicola et al., 2006; Xiang and Vlassak, 2006). These two opposite thickness effects are mainly as a result of the great difference between the surface-constraints of thin films. In the thin films without surface treatment, the free surface-constraint is much weaker than the interior GB-constraint and the dislocations in surface grains could exit easily from the free surfaces. As a result, the surface grains are much easier to deform plastically than the interior grains. However, in the thin films with SPLs, dislocations nucleated in the surface grains are blocked by SPLs and accordingly the surface grains are relatively hard to deform plastically. With the decrease of film thickness, the percentage of the surface grains in all grains increases and the surface-constraint would make a more significant contribution to the tensile strength of polycrystalline thin films. Hence, two opposite thickness effects induced by different surface-constraints are actually attributed to the competition between the exterior surface-constraint and interior GB-constraint. According to this point of view, besides surface passivation, other surface treatments, such as surface grain refinement, may also significantly influence the tensile strength of thin films and induce thickness effects. Therefore, an accurate understanding of the thickness effects induced by various surface micro-treatments is indispensable for the micro-manufacturing/processing of thin films.

In the past two decades, several computational tools have been developed to understand the size dependent behavior of materials at the micron/nanometer scale. Therein, discrete dislocation dynamics (DDD) is believed to be one of the most efficient numerical methods to capture the size dependent plasticity at the micron scale (Akarapu et al., 2010; Deshpande et al., 2005; Guruprasad and Benzerga, 2008; Kumar et al., 2009; Nicola et al., 2003, 2005a; Ouyang et al., 2010; Shishvan et al., 2011; Tang et al., 2007). As is well known, GBs act as main obstacles to the movements of dislocations in polycrystalline materials. The penetrability of GBs for dislocations directly controls the micro-plasticity within grains and thus influences the overall response of polycrystalline materials to the applied loading (Kumar et al., 2010; Shen et al., 1986, 1988). However, in most of the existing DDD simulations of polycrystalline materials, GBs are usually treated as impenetrable boundaries (Balint et al., 2008; Espinosa et al., 2006; Nicola et al., 2006; Ouyang et al., 2008). This simple treatment overestimates the constraint of GBs on the movements of dislocations and may lead to inaccurate predication of size effects.

As is mentioned above, the mechanical behavior of polycrystalline thin films, although they are subjected to simple pure tension, is very complicated, depending upon not only the film thickness and grain size, but also the percentage of surface grains in total grains and the size ratio of surface grains to interior grains. In the complicated thickness dependent behavior, the competition between the exterior surface-constraint and interior GB-constraint plays a very important role (Bayley et al., 2007; Geers et al., 2007, 2006). Motivated by this background, we employ the two-dimensional DDD framework of Van der Giessen and Needleman (1995) to study the thickness dependent behavior of polycrystalline thin films with penetrable GBs. Besides, the penetrable GB model advanced by Hou et al. (2009) and Li et al. (2009) is incorporated into the DDD framework to take into account dislocation penetration through GBs and dislocation emission from GBs. In this work, we mainly investigate how the competition between the exterior surface-constraint and interior GB-constraint influences the overall tensile strength of polycrystalline thin films, with special focus on the thickness effect. Considering the grain size effect (i.e., Hall–Petch relation) has been extensively studied heretofore, the grain size in all polycrystalline thin films remains unchanged in our computations to avoid the mutual interference between thickness effect and grain size effect.

This paper is organized as follows. The computational models and the adopted numerical methodology are introduced briefly in Section 2. Section 3 provides the main results and in-depth discussions. In Section 4, some concluding remarks end this paper.

2. Computational model and methodology

2.1. Computational model

Three types of thin films, including the thin films (a) without surface treatment, (b) with SPLs of nanometer thickness and (c) with surface grain refinement zones (SGRZs) consisting of nano-sized grains, are selected to study thickness effect on the tensile strength of thin films, as are sketched in Fig. 1. Only two-dimensional polycrystalline thin films are considered in this work for simplicity. Since thickness effects are the major topic in this paper, the length of each film is kept constant, i.e., $L = 4.5$ μm. In order to mimic the realistic geometrical details of grains in polycrystalline thin films, the well-known Voronoi polygon is adopted to generate all the grains, with the mean sizes of each grain in both the length and thickness directions of films being approximately equal, denoted as d. In the films without surface treatment, all the mean sizes of grains are approximately the same as shown in Fig. 1(a). In the films with SPLs, two passivation layers, which are 10 nm thick and comparable with the passivation layers adopted in the experiment of Xiang et al. (2006), are perfectly bonded on the bottom and top surfaces as shown in Fig. 1(b). In order to model surface grain refinement, each surface grain whose mean size is the same as that of the interior grains (about 0.25 μm) is further refined into 16 smaller nano-sized grains as shown in Fig. 1(c). As an approximation, the elastic behavior of all the grains and SPLs is assumed to be isotropic (Espinosa et al., 2006; Nicola et al., 2005a, 2006) with Young's modulus $E = 70$ GPa and Poisson's ratio $\nu = 0.33$. The anisotropy of grains can be depicted by a certain number of slip systems with given spatial orientations. As we know, FCC grain commonly has 12 possible slip systems, consisting of four slip planes $\{1\ 1\ 1\}$ and three slip directions $\langle 1\ 1\ 0\rangle$ on each slip plane. However, for the present 2D plane strain model, only two slip systems with crossing angle of 60° are considered in each grain for simplicity. Although the slip systems in each grain are randomly orientated, the misorientation of slip systems between two adjacent grains is especially limited within the range of $0–2\Delta\theta$. Without loss of generality, the mean GB misorientation $\Delta\theta$ is typically set as 7.5°. Actually, there exist many potentially active slip planes in each slip system. In the present computations, the space between adjacent slip planes is typically set to be $150b$, where $b = 0.25$ nm is the magnitude of the Burgers vector.

Because the deformation field within dislocation core is singular, those slip planes intersecting either of two ends of films are not considered in the computational models to avoid numerical complication. Only the Frank–Read dislocation nucleation mechanism is simulated in the studied films. A quantity of dislocation sources with the density of $\rho_{src} = 50\ \mu m^{-2}$ are randomly dispersed on those potentially active slip planes. The strength τ_{nuc} of individual dislocation source is randomly assigned, following the

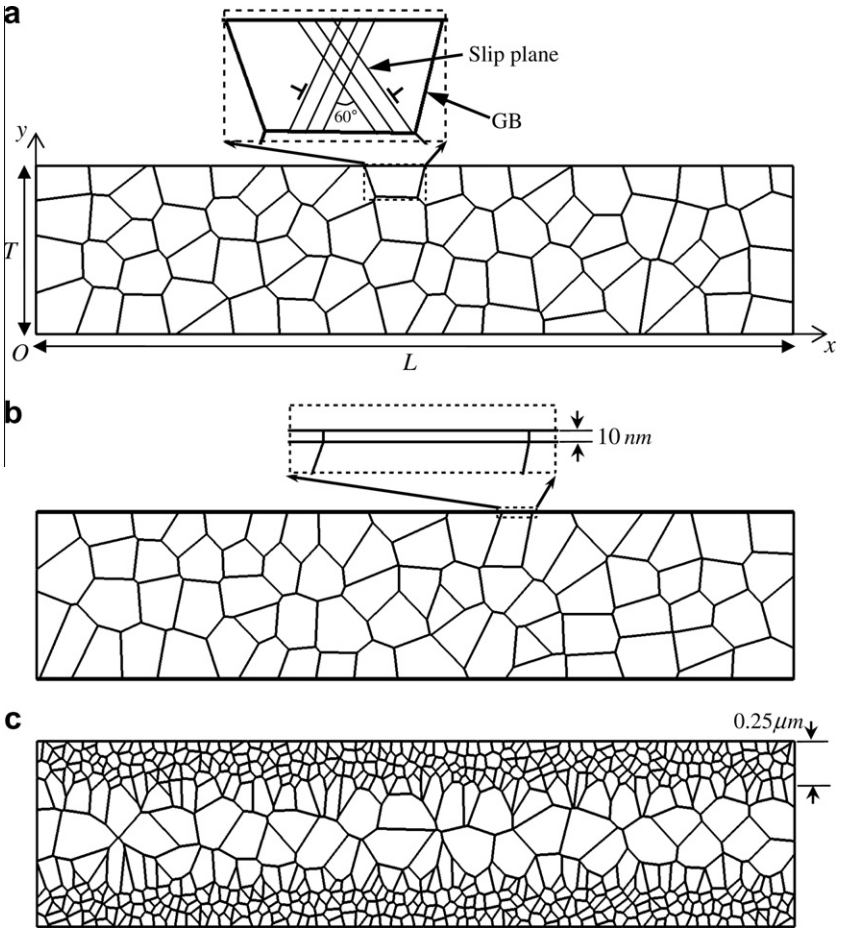

Fig. 1. Sketches of three types of polycrystalline thin films: (a) without surface treatment, (b) with SPLs and (c) with SGRZs.

Gaussian distribution with mean 50 MPa and variance 10 MPa, which are the same as the empirical values adopted by the previously published literature (Van der Giessen and Needleman, 1995).

In the computation, uniaxial tension is applied at two ends of films with displacement control as follows:

$$\Delta U_x = \begin{cases} -\dot{\varepsilon}\Delta t L/2 & \text{at } x = 0 \\ \dot{\varepsilon}\Delta t L/2 & \text{at } x = L \end{cases} \tag{1}$$

where $\dot{\varepsilon}$ is the applied strain rate, L is the length of each film and Δt (Δt = 0.5 ns) is the time step increment. In order to reduce computation cost, a relatively high strain rate of $\dot{\varepsilon} = 2000\ \text{s}^{-1}$ is adopted in the computation, and all the films are tensioned to ε = 1.0%.

The tensile stress σ, which is the overall response of thin films to the applied strain ε, can be approximatively calculated by:

$$\sigma = \frac{1}{T}\int_0^T \sigma_x(L, y)dy \tag{2}$$

where T is the thickness of each film.

2.2. Discrete dislocation dynamics (DDD) framework

At the beginning of DDD computation, the polycrystalline thin film is assumed to be dislocation-free. With the increase of tensile strain, two oppositely signed dislocations, with the critical distance $L_{nuc} = Eb/[4\pi(1-\nu^2)\tau_{nuc}]$, are nucleated at certain Frank–Read source once the resolved shear stress acting on it exceeds the critical strength τ_{nuc} and persists for a period of time t_{nuc} = 10 ns (Van der Giessen and Needleman, 1995). After N dislocations nucleated, the Van der Giessen–Needleman's superposition scheme should be adopted to calculate the displacement, strain and stress fields ($\mathbf{u}$, $\boldsymbol{\varepsilon}$, $\boldsymbol{\sigma}$) in the film as follows:

$$\boldsymbol{u} = \tilde{\boldsymbol{u}} + \hat{\boldsymbol{u}}; \quad \boldsymbol{\varepsilon} = \tilde{\boldsymbol{\varepsilon}} + \hat{\boldsymbol{\varepsilon}}; \quad \boldsymbol{\sigma} = \tilde{\boldsymbol{\sigma}} + \hat{\boldsymbol{\sigma}} \tag{3}$$

In this scheme, the singular fields $\tilde{}$, which are associated with N dislocations occupying their respective positions in the polycrystalline film, can be calculated by summing up the analytical fields of N dislocations in an infinite solid. For the present boundary value problem of the thin film, the image fields $\hat{}$, which can be easily solved with the linearly elastic finite element method (FEM), must be superposed as supplemental fields in order to modify the continually changing boundary condition induced by the dynamical evolvement of dislocation pattern in the film.

Under the joint action of the stress field $\sum_{J\neq I}\boldsymbol{\sigma}^J$ exerted by other $(N-1)$ dislocations and the image stress field $\hat{\boldsymbol{\sigma}}$, the Peach–Koehler force acting on the dislocation I can be calculated by (Van der Giessen and Needleman, 1995)

$$f^I = \boldsymbol{m}^I \cdot \left(\sum_{J\neq I}\boldsymbol{\sigma}^J + \hat{\boldsymbol{\sigma}}\right) \cdot \mathbf{b}^I, \tag{4}$$

where $\mathbf{m}^I$ is the unit vector normal to the slip plane on which the dislocation I locates and $\mathbf{b}^I$ the Burgers vector of the dislocation I. Driven by the Peach–Koehler force f^I, the dislocation I glides with the velocity $v^I = f^I/B$ (Cleveringa et al., 1999), with the drag coefficient B usually set as 10^{-4} Pa s (Kubin et al., 1992). As suggested by Cleveringa et al. (1999), a truncated dislocation velocity of 20 m/s is adopted in order to avoid the computational instability. Two dislocations with opposite signs annihilate when they

approach each other within the critical distance of $L_a = 6b$. Only the skeleton of the 2D-DDD framework is briefly recalled here for the convenience of readers. More details can be found elsewhere (Cleveringa et al., 1999; Deshpande et al., 2005; Van der Giessen and Needleman, 1995).

2.3. Dislocation-GB interaction model

In order to study the mechanical behavior of polycrystalline materials with penetrable GBs, a 2D dislocation-GB interaction model is proposed by Hou et al. (2009) and Li et al. (2009) and has been further incorporated into the Van der Giessen–Needleman's 2D-DDD framework. For the convenience of readers, the two main scenarios involved in this model are briefly overviewed in the following two subsections. More details about this model can be found in the literatures (Hou et al., 2009; Li et al., 2009).

2.3.1. Dislocation penetration through GBs

Without loss of generality, two adjacent grains sharing GB l are schematized in Fig. 2(a). Driven by the Peach–Koehler force f^A, the dislocation A glides towards the GB l on its own ship plane S_1. Due to the strong constraint from the GB l, the dislocation A is pinned in front of the GB l. With the increase of applied loading, a growing number of dislocations nucleate from their sources and then glide towards the GB l and increasingly pile up at the rear of the head dislocation A, rendering the stress concentration at the GB to continually increase. Once this concentrated stress exceeds the GB strength τ_{pass}:

$$\tau_{\text{pass}} = (E_{GB}b_A + \alpha G\Delta b^2)/b_A^2 \tag{5}$$

where E_{GB}, $\alpha = 0.5$ (Hull and Bacon, 2001) and G are the GB energy density, material constant and shear modulus, respectively, the head dislocation A penetrates through the GB l into the grain B in the most energy-saving manner and synchronously leaves dislocation debris with the Burgers vector $\Delta b = b_A - b_B$ on the GB l (Shen et al., 1986, 1988). The GB energy density E_{GB}, which is closely related to the crystallographic misorientation $\delta\theta$ between grains A and B, can be simply expressed as (Hasson and Goux, 1971)

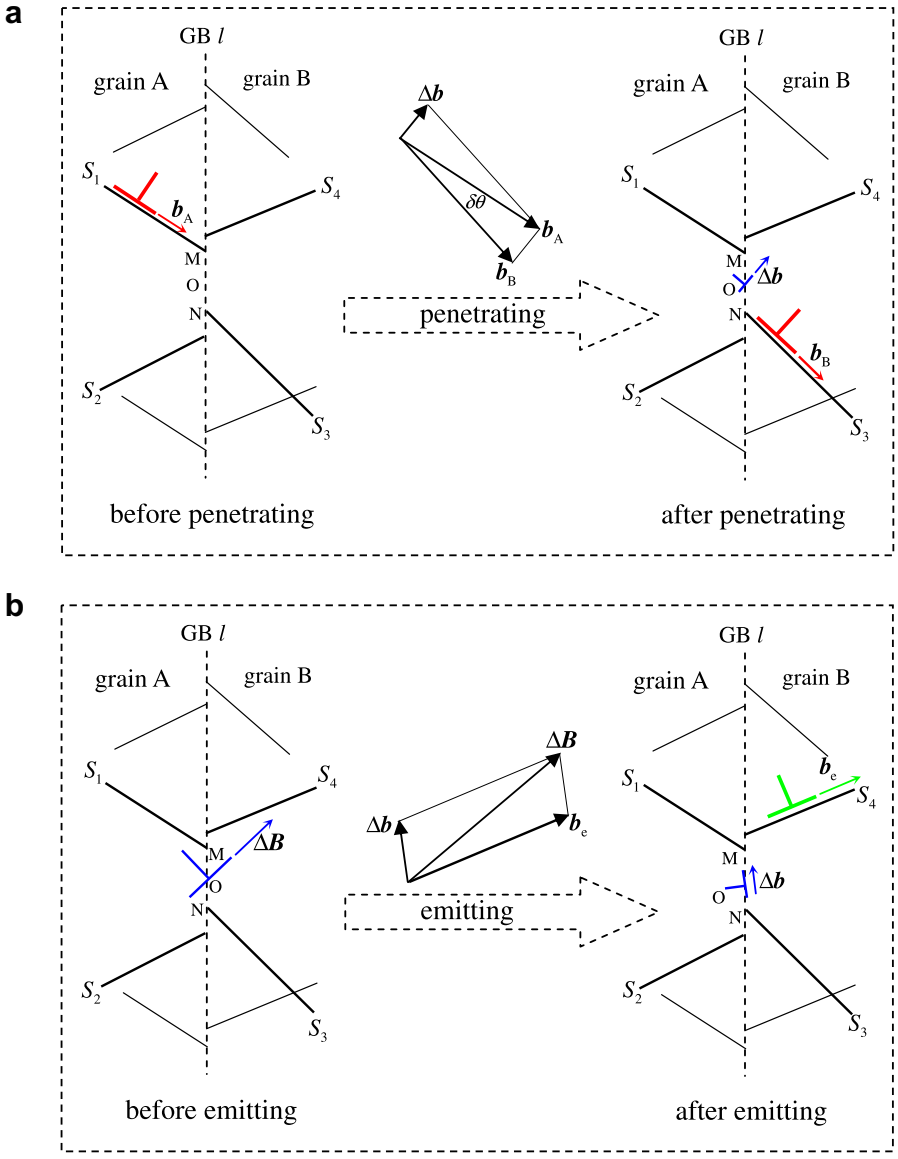

Fig. 2. Schematic of the dislocation-GB interaction model: (a) dislocation penetrating through GB and (b) dislocation debris emitting a perfect dislocation. The "⊥" symbols on GBs and on slip planes denote dislocation debris and perfect dislocations, respectively.

$$E_{GB}=\begin{cases} k\delta\theta/\theta_1, & 0\leqslant\delta\theta<\theta_1 \\ k, & \theta_1\leqslant\delta\theta<\theta_2 \\ k(\pi/2-\delta\theta)/(\pi/2-\theta_2), & \theta_2\leqslant\delta\theta<\pi/2 \end{cases} \quad (6)$$

where $\theta_1\approx\pi/9$, $\theta_2\approx 8\pi/9$ and $k\approx 0.6\,\mathrm{J/m^2}$ for polycrystalline aluminum (Hasson and Goux, 1971).

2.3.2. Dislocation emission from GBs

With the increase of the number of dislocation penetration events, dislocation debris continually accumulates into large dislocation debris $\Delta\mathbf{B}$ on the GB l as illustrated in Fig. 2(b), rendering the continual increase of the dislocation debris energy. In order to release the energy of dislocation debris, a new perfect dislocation $\mathbf{b}_e$ is emitted from $\Delta\mathbf{B}$, leaving new dislocation debris $\Delta\mathbf{b}'=\Delta\mathbf{B}-\mathbf{b}_e$ on the GB l. Whether or not the dislocation debris $\Delta\mathbf{B}$ can successfully emit a perfect dislocation and which slip plane is chosen by the dislocation $\mathbf{b}_e$ as its outgoing slip plane depend on the following three criteria: (1) the magnitude of $\Delta\mathbf{B}$ must be greater than or equal to that of one perfect dislocation; (2) dislocation emission must be energetically favorable; (3) if more than one slip plane satisfy both the criteria (1) and (2), the slip plane, on which the resolved shear stress is the highest, is usually selected by the dislocation $\mathbf{b}_e$ as its outgoing slip plane.

3. Results and discussion

In this section, the thickness dependent behavior of polycrystalline thin films is computationally studied, with focus on the competition between the exterior surface-constraint and interior GB-constraint. Firstly, the thickness effect on the tensile strength of polycrystalline thin films without surface treatment and its intrinsic dislocation mechanism attract our special attention. For the sake of comparison, the influence of two kinds of surface treatments on the thickness effect is also discussed, including surface passivation and surface grain refinement.

In all computations, in order to mimic the micro-structures of polycrystals as close as possible, we randomly assigned the locations of grain seeds in Voronio's method, the orientations of slip systems in each grain, as well as the strengths and locations of dislocation sources. To reduce the influence of random factors as much as possible, we repeat all the following computations three times with different random assignments, and plot all the curves with the arithmetic average of these repeatedly computed results. The error bars are not plotted in the following figures for the sake of clarity.

3.1. Thickness effect of polycrystalline thin films without surface treatment

For the convenience of comparison, six thin films with different thicknesses, i.e., 0.25 μm, 0.5 μm, 0.75 μm, 1.0 μm, 1.25 μm and 1.5 μm, are studied, respectively. The mean grain size of all films is assumed to remain unchanged (i.e., $d=0.25$ μm) to avoid the disturbance from the grain size effect. There are 18 grains in the length direction and about 1–6 grains in the thickness direction of films, depending on the film thickness.

Fig. 3 plots the stress–strain curves of six films with different thicknesses. It can be easily seen from Fig. 3 that with the increase of film thickness, the tensile strength remarkably increases, especially when the film thickness T is not larger than 1.0 μm or the number of grains in the thickness direction (T/d) is not more than 4. Once the film thickness T is larger than 1.0 μm or $T/d>4$, the thickness effect on the stress–strain response becomes weak or even negligible. One the other hand, when the number of grains in the thickness direction is 1 or 2 and thus all grains are surface

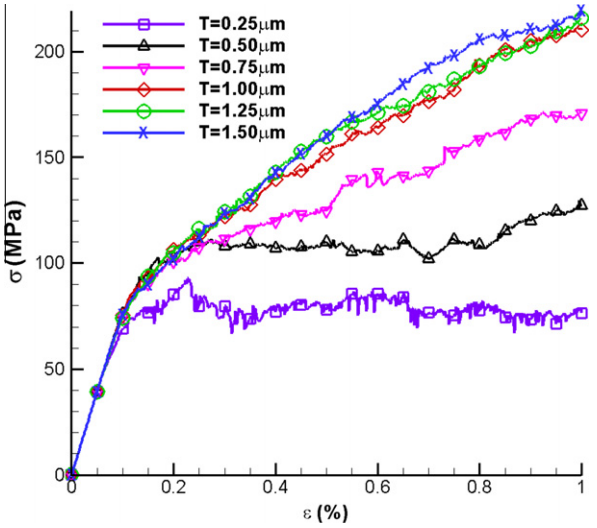

Fig. 3. Stress–strain response of the films without surface treatment with different thicknesses.

grains, the strain hardening rate ($d\sigma/d\varepsilon$) is very low. Once the number of grains in the thickness direction is more than 2, some of which are interior grains, the strain hardening rate becomes high. This means that there is a great change in the strain hardening mechanism when the interior grains appear, which may originate directly from the GB-constraint of interior grains on gliding dislocations. Moreover, Fig. 4 plots the variations of the tensile strengths at different strains (i.e., 0.2%, 0.6% and 1.0%) with T/d. Two distinct features could be seen from Fig. 4: (I) the thickness effect on the tensile strength at the strain of 0.2% is weak or even negligible; (II) with the increase of applied strain, the thickness effect on the tensile strengths (such as $\sigma_{0.6\%}$ or $\sigma_{1.0\%}$) is strong when $T/d\leqslant 4$ but almost disappears when $T/d>4$. Obviously, there exists a critical grain number ($T/d\approx 4$) in the thickness direction, below which the thickness effect is strong but above which the thickness effect gradually becomes weak or even disappears. This critical grain number ($T/d\approx 4$), which seems to be independent of the materials, thicknesses and grain sizes of thin films, was also experimentally observed by several groups (Geers et al., 2006; Keller et al., in press; Miyazaki et al., 1979). These interesting thickness

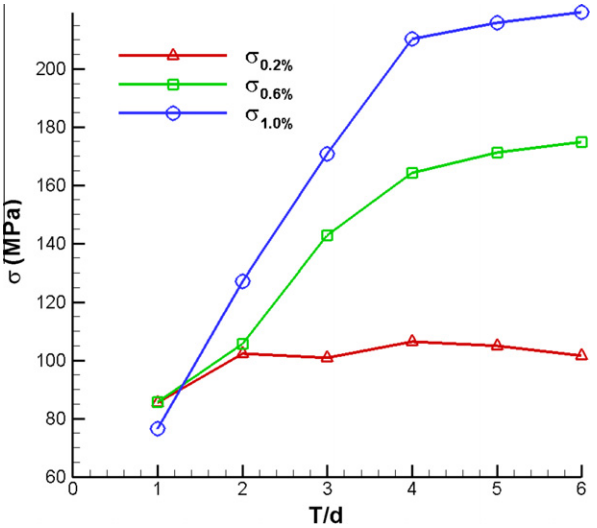

Fig. 4. Variations of the tensile strengths at different strains with T/d for thin films without surface treatment.

effects can be briefly explained as follows. When the number of grains in the thickness direction is only 1 or 2, nucleated dislocations in all surface grains can easily glide out from the film surfaces. Accordingly, the overall tensile stress of thin film is low. When the grain number increases to 3 or 4, interior grains appear in the polycrystalline films. The interior grains are harder than the surface grains because the interior GB-constraint is stronger than the exterior free surface-constraint, rendering the increase of overall tensile strength with increasing film thickness. Obviously, the thickness effect of "thicker is stronger" is due to the competition between the exterior surface-induced weakening and interior GB-induced strengthening (Geers et al., 2006). If the number of interior grains increases further, the interior GB-induced strengthening gradually exceeds the exterior surface-induced weakening, so the thickness effect gradually disappears. The present computational results are in qualitative agreement with the existing experimental results (Geers et al., 2006; Keller et al., in press; Miyazaki et al., 1979). It is worth specially noting that the present thickness effect (i.e., "thicker is stronger") is reasonable only when the grain size remains unchanged. If the grain size decreases with decreasing film thickness, the interior GB-induced strengthening effect (i.e., grain size effect or Hall–Petch effect) dominates the stress–strain response of polycrystalline thin films; maybe an opposite thickness effect arises (Xiang and Vlassak, 2006).

To further explain the underlying dislocation mechanism behind the thickness effect displayed in Figs. 3 and 4, all films with different thicknesses are averagely subdivided into 30 sheets in the thickness direction and the average dislocation density in each sheet is denoted as ρ_s. The through-thickness distributions of ρ_s in six films at the strain of 0.2% are plotted in Fig. 5. All the films are still at or just beyond the initial yield stage at this low strain level, and only a few dislocation sources could nucleate dislocations due to the lower resolved shear stresses acting on them. Consequently, the dislocation densities in both surface grains and interior grains are very low as shown in Fig. 5. Since the applied stress and the dislocation density are low, the Peach–Koehler force acting on dislocations and thus the dislocation velocity are also low. Only a few dislocations could successfully penetrate through GBs or exit from the surfaces, and therefore most of them still glide within their own grains. In other words, the dislocation density difference between the surface grains and interior grains is small at lower strain, as can be seen in Fig. 5, thereby the contribution of the surface grains to the overall tensile strength is almost the same as that of the interior grains. As a result, negligible thickness effect is observed in Figs. 3 and 4 at the strain of 0.2%.

The through-thickness distribution of ρ_s at $\varepsilon = 1.0\%$ is plotted in Fig. 6. The dislocation pattern and contour of tensile stress σ_x at $\varepsilon = 1.0\%$ are given in Fig. 7. It is clear that there are great differences in the dislocation pattern and stress distribution of six films with different thicknesses. In the thinnest 2 films with $T = 0.25$ μm and $T = 0.5$ μm, where there is only 1 or 2 grains in the thickness direction, only a few dislocations stay in these surface grains. This is believed to be associated with easy exit of nucleated dislocations from the free surfaces of thin films due to the weak surface-constraint. In the 2 films with middle thicknesses of 0.75 μm and 1.0 μm, there exist 3 or 4 grains in the thickness direction and about one-third or half are interior grains. Because the remarkable difference between the exterior free surface-constraint and interior GB-constraint on gliding dislocations, those dislocations in surface grains are easy to exit but those in interior grains are hampered by GBs; thus the dislocation density and tensile stress σ_x in interior grains are much higher than those in surface grains, as shown in Figs. 6(a) and 7(c) and (d). Compared with the weak exterior free surface-constraint, the strong interior GB-constraint contributes much to the overall tensile strength. This follows that in the polycrystalline films containing 3 or 4 grains in the thickness direction,

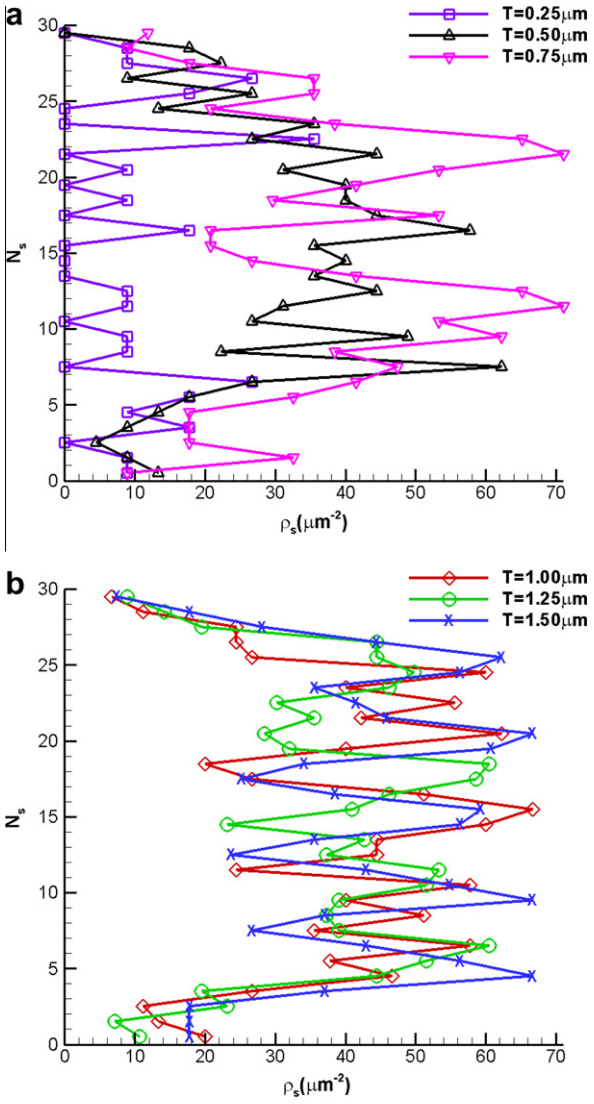

Fig. 5. Through-thickness distribution of ρ_s at $\varepsilon = 0.2\%$ in the films with different thicknesses: (a) $T = 0.25$, 0.50, 0.75 μm and (b) $T = 1.00$, 1.25, 1.50 μm.

thickness effect mainly originates from the competition between weakening effect induced by exterior free surface-constraint and strengthening effect induced by interior GB-constraint (Geers et al., 2006). With the increase of film thickness, the percentage of interior grains in total grains increases and therefore the strengthening effect resulting from interior GB-constraint enhances, displaying "thicker is stronger". Further, when the film thickness is larger than 1.0 μm with more than 4 grains in the thickness direction, the interior grains are in the majority. Figs. 6 and 7(e) and (f) show clearly that, in these thicker films, the dislocation density and tensile stress σ_x within the interior region are much higher than those in the region near surfaces, and the high stress region is greatly larger than the low stress region. It is easy to understand that, in thicker films, the strengthening effect induced by the interior GB-constraint substantially prevails against the weakening effect induced by the exterior free surface-constraint and dominates the overall tensile strength. In other words, for the thicker film, its overall tensile strength is mainly dominated by the interior penetrable GB-constraint, which depends on grain size rather than film thickness. In all our computations, the grain size always remains unchanged; accordingly, the thickness effect gradually vanishes when $T/d > 4$, as shown Figs. 3 and 4.

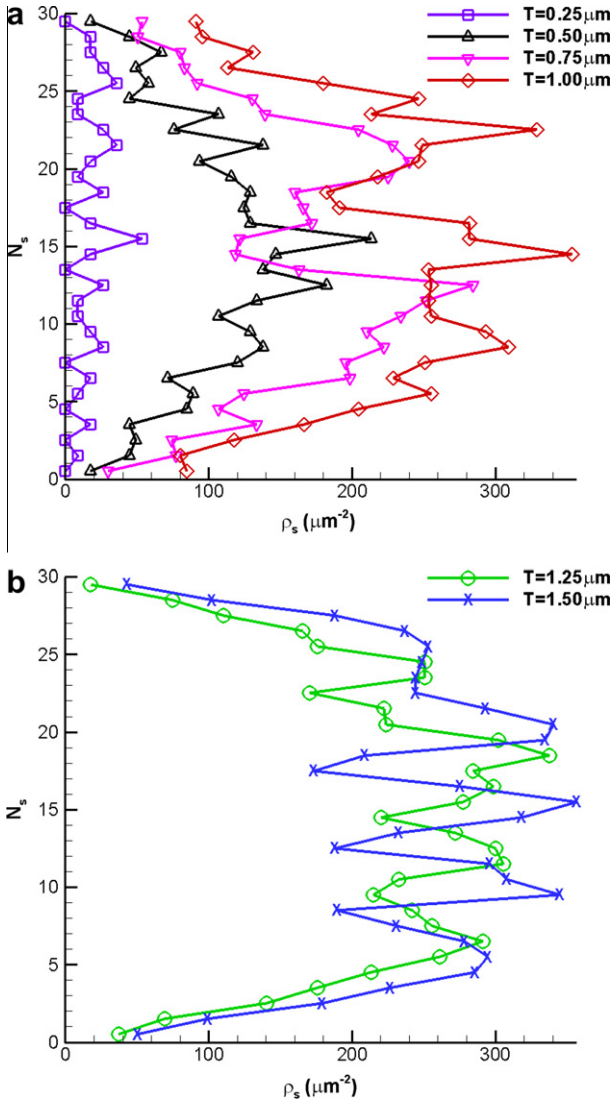

Fig. 6. Through-thickness distribution of ρ_s at $\varepsilon = 1.0\%$ in the films with different thicknesses: (a) $T = 0.25, 0.50, 0.75, 1.00\ \mu m$ and (b) $T = 1.25, 1.50\ \mu m$.

3.2. Thickness effect of polycrystalline thin films with SPLs

In order to further discuss the key role of the competition between exterior surface-constraint and interior GB-constraint in the thickness effect, in this subsection, the tensile behavior of thin films with SPLs is studied. Two passivation layers of 10 nm thickness, which are impenetrable by dislocations, are perfectly bonded to the bottom and top surfaces of films, as illustrated in Fig. 1(b). For simplification, the SPLs are assumed to be the same as the films in material parameters. The thickness and mean grain size of six films considered in this subsection are the same as those in Section 3.1 for the sake of comparison.

The stress–strain curves of polycrystalline thin films with SPLs are plotted in Fig. 8. We can see that there is strong thickness effect on the stress–strain curves, especially at larger strain. However, different from the thickness effect of films without surface treatment, the tensile strength of films with SPLs increases with decreasing film thickness, i.e., "thinner is stronger". At the lower strain, the thickness effect is weak or even negligible and similar to that of films without surface treatment.

In Fig. 9, the variations of the tensile strengths at different strains with T/d for the thin films with and without SPLs are plotted together for the purpose of comparison. For passivated thin films, careful comparison between our computations and Xiang et al.'s experiments (2006) reveals both qualitative agreement and quantitative difference. Both our computations and their experiments show the tensile strength of thin films with SPLs decreases with the increase of T/d; however, there is visible difference in quantity between them. This is mainly because different material parameters and micro-structures are chosen in two works. In addition, we can see from Fig. 9 that, at the low strain of 0.2%, there is insignificant difference between the tensile strengths of the passivated and unpassivated films. At the strain of 0.2%, few dislocations exit from the free surfaces in the unpassivated films or are blocked by the SPLs in the passivated films, so the influences of free surfaces and SPLs on the tensile strength are insignificant in fact. With the increase of applied strain, opposite thickness effects could be clearly seen in Fig. 9 for the passivated and unpassivated films. When T/d increases and $T/d \leqslant 4$, the overall tensile strength at larger strain (such as $\varepsilon = 0.6\%$ or $\varepsilon = 1.0\%$) increases for the unpassivated films but decreases for the passivated films. Once $T/d > 4$, both opposite thickness effects gradually vanish. Why do opposite thickness effects arise in passivated and unpassivated films? In order to answer this interesting question, the through-thickness distribution of ρ_s at $\varepsilon = 1.0\%$ in six passivated films with different thicknesses is showed in Fig. 10. It can be easily seen that dislocation density sharply increases near the film-passivation interfaces due to the strong SPL-constraint on gliding dislocations, which is distinctly different from that in the unpassivated films where dislocation density sharply decreases near the surfaces because of the weak surface-constraint as shown in Fig. 6. If we make a careful comparison between Figs. 6 and 10(a), it can be found that, the magnitude of the dislocation densities in the interior grains of the passivated and unpassivated films are about the same, i.e., about 250 μm^{-2}. This is mainly because all GB misorientation is assigned with the same method and thus all GB strengths are almost the same. It is clear that above mentioned opposite thickness effects mainly arise from the opposite dislocation density gradients near the passivated surfaces and unpassivated surfaces. The variation of ρ_s with the distance d_p from the bottom film-passivation interface is especially magnified in Fig. 10(b). We can find that in the region near the film-passivation interface, there is a boundary layer, within which the dislocation density sharply increases and is much higher than that in the interior region of film. This boundary layer thickness is about 75 nm and independent of film thickness, showing good agreement with the strain gradient plasticity prediction and experiment (Nicola et al., 2006; Xiang and Vlassak, 2006). As is well known, plastic strain mainly comes of the movements of dislocations. Within these boundary layers, the plastic strain is difficult to develop due to the severe dislocation pileup; as a result, the stress is high there in order to accommodate the applied tensile strain, as displayed in Fig. 11. Accordingly, in the passivated films, the exterior passivated surface-constraint induces strengthening to the overall tensile strength but the interior GB-constraint acts as relative weakening. When the film thickness increases but $T/d \leqslant 4$, the percentage of boundary layers decreases because their thicknesses are independent of the film thickness; thereby the strengthening effect induced by the boundary layers decreases and the weakening effect by relatively softer interior GB-constraints increases. So it is not surprising that the thicker film is weaker. With the film thickness increasing further and $T/d > 4$, the interior GB-constraint substantially prevails against the exterior passivated surface-constraint; as a result, the overall strength of thin films is mainly dominated by those interior grains and the thickness effect gradually vanishes.

In order to highlight the contribution of GB characterization, the overall tensile strengths of the passivated-films with impenetrable GBs and penetrable GBs are plotted in Fig. 12. It is clear that strong

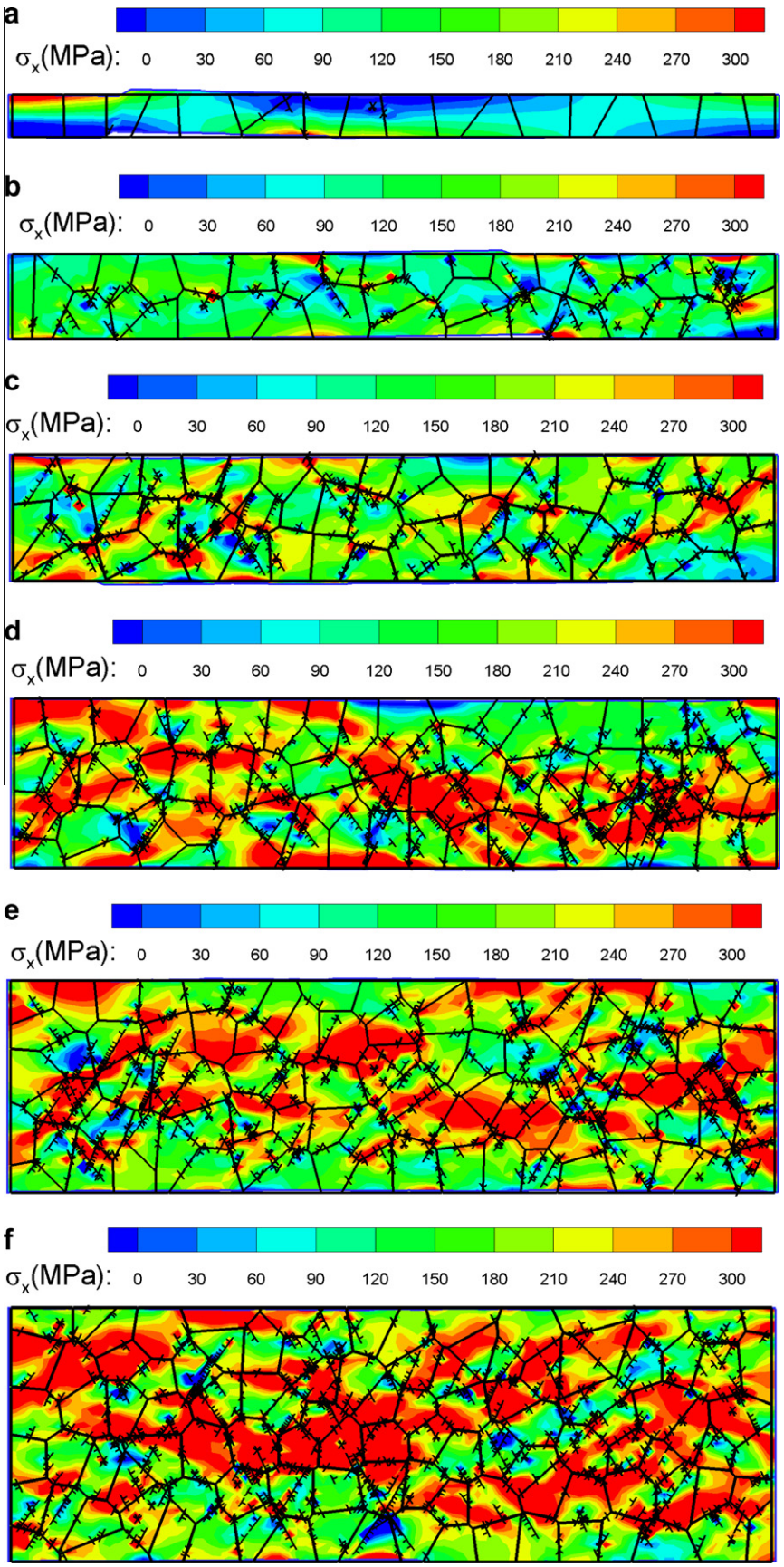

Fig. 7. Dislocation pattern and contour of tensile stress σ_x at $\varepsilon = 1.0\%$ in the films with different thicknesses: (a) $T = 0.25$ μm, (b) $T = 0.50$ μm, (c) $T = 0.75$ μm, (d) $T = 1.00$ μm, (e) $T = 1.25$ μm and (f) $T = 1.50$ μm. The symbols "⊥" represent dislocations.

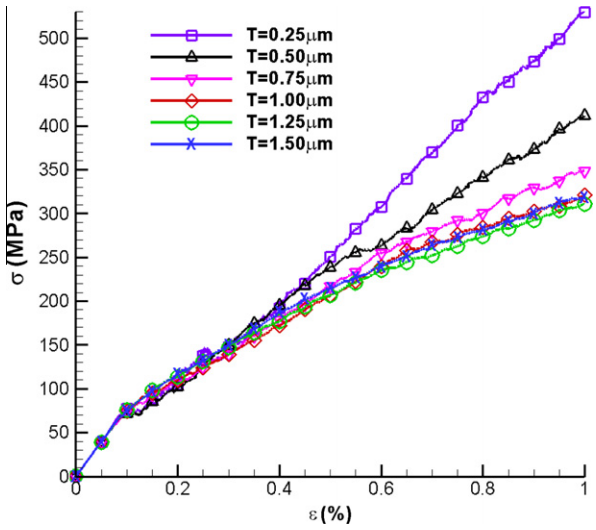

Fig. 8. Stress–strain response of the films with SPLs with different thicknesses.

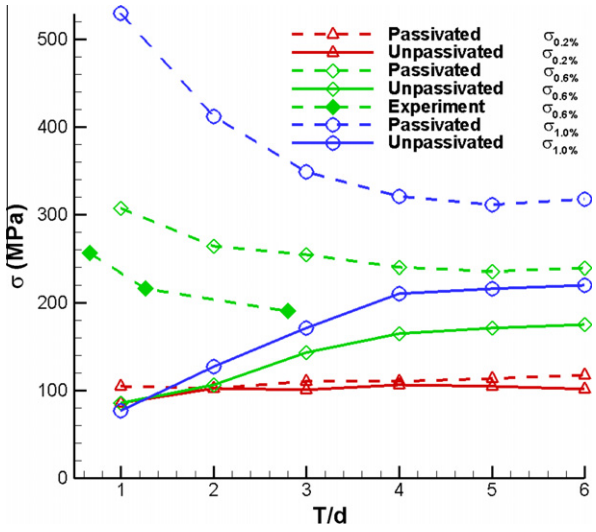

Fig. 9. Variations of the tensile strengths at different strains with T/d for passivated and unpassivated films. The experiment curve is the variation of the tensile strength at $\varepsilon = 0.6\%$ for films with SPLs (Xiang and Vlassak, 2006).

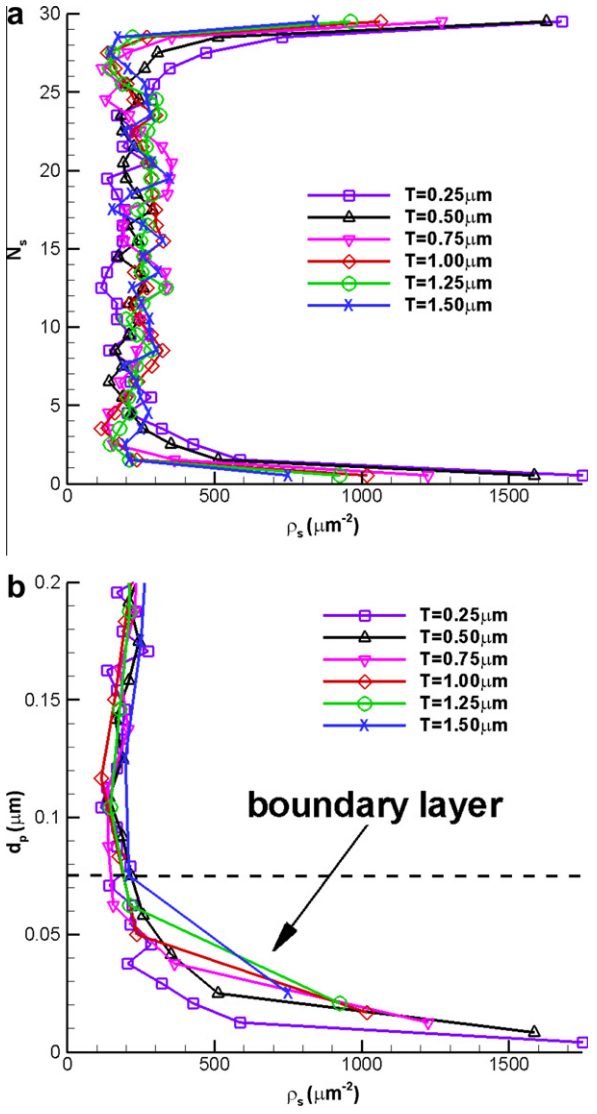

Fig. 10. (a) Through-thickness distribution of ρ_s at $\varepsilon = 1.0\%$ and (b) distribution of ρ_s at $\varepsilon = 1.0\%$ near the bottom film-passivation interface.

thickness effect on the tensile strengths $\sigma_{0.6\%}$ and $\sigma_{1.0\%}$ is captured by the present penetrable GB model, but negligible thickness effect is predicted by the impenetrable GB model. This is mainly because the treatment of impenetrable GBs overestimates the GB-constraint on dislocations in grains; so all dislocations in interior grains are blocked by GBs. In this situation, the constraint strengths of SPLs and interior GBs are about at the same level. As we pointed out above, the thickness effect mainly arises from the competition between the exterior surface-constraint and interior GB-constraint. Since this competition does not exist in the surface-passivated polycrystalline thin films containing impenetrable GBs, it is not surprising that negligible thickness effect is predicted.

3.3. Thickness effect of polycrystalline thin films with SGRZs

In the actual application of thin films, in addition to surface passivation, surface grain refinement is also a popular method to enhance the strength of films. In order to understand the thickness effect of polycrystalline thin films with SGRZs, in this subsection, four films with thickness of 0.75 μm, 1.0 μm, 1.25 μm and 1.5 μm are comparatively investigated. To simulate the surface grain refinement, the mean size of all interior grains is still 0.25 μm, but each surface grain is roughly subdivided into 16 nano-sized grains with the mean size of about 60 nm as shown in Fig. 1(c).

The stress–strain curves of polycrystalline thin films with SGRZs are plotted in Fig. 13. It is clear that the overall tensile strength of thin films decreases with increasing film thickness, displaying "thinner is stronger". Seemingly, the thickness effect of the films with SGRZs is the same as that of the films with SPLs. However, the underlying dislocation mechanisms behind them are different. This can be clearly seen from Fig. 14, where the through-thickness distribution of ρ_s at $\varepsilon = 1.0\%$ is plotted. In the SGRZs, those refined grains are so small (about 60 nm) that dislocations are difficult to nucleate; to accommodate the applied strain, the stress achieved there is higher than that in those interior grains, as shown in Fig. 15. In the thinner films, the higher stress region within SGRZs makes a chief contribution to the overall tensile strength. With the increase of film thickness, the percentage of SGRZs decreases, leading to the thickness effect of "thinner is stronger" as shown in Fig. 13. If the film thickness increases further and becomes large enough, the contribution of the low stress region in interior grains

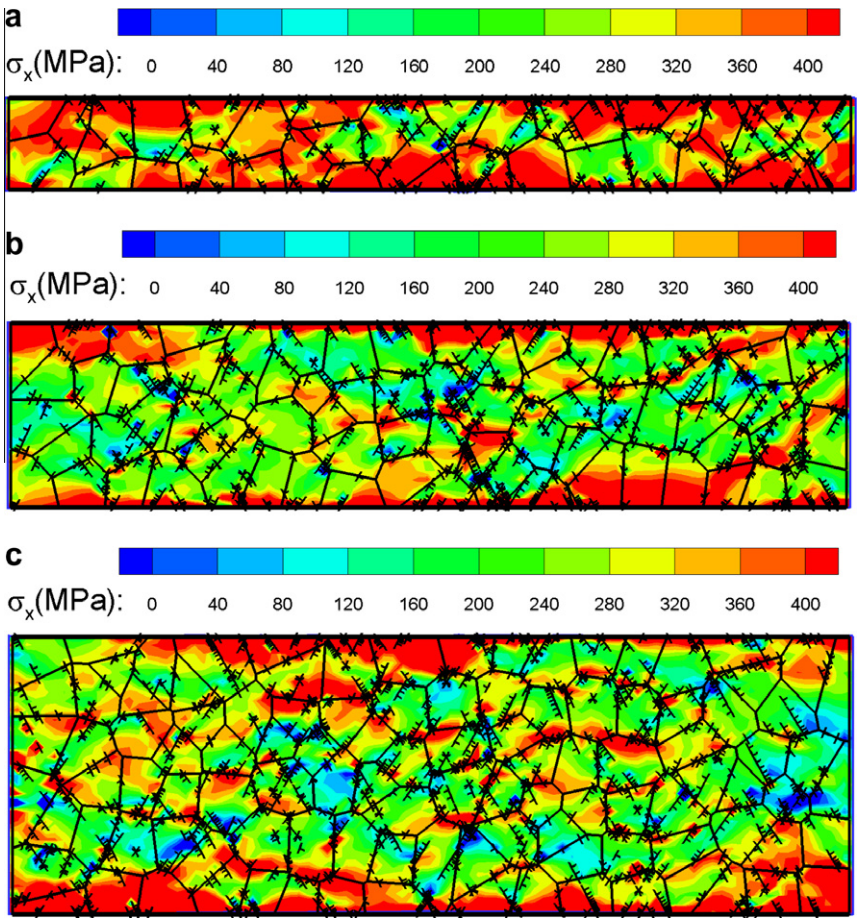

Fig. 11. Dislocation pattern and contour of tensile stress σ_x at $\varepsilon = 1.0\%$ in the films with different thicknesses: (a) $T = 0.50$ μm, (b) $T = 1.00$ μm and (c) $T = 1.50$ μm. The symbols "⊥" represent dislocations.

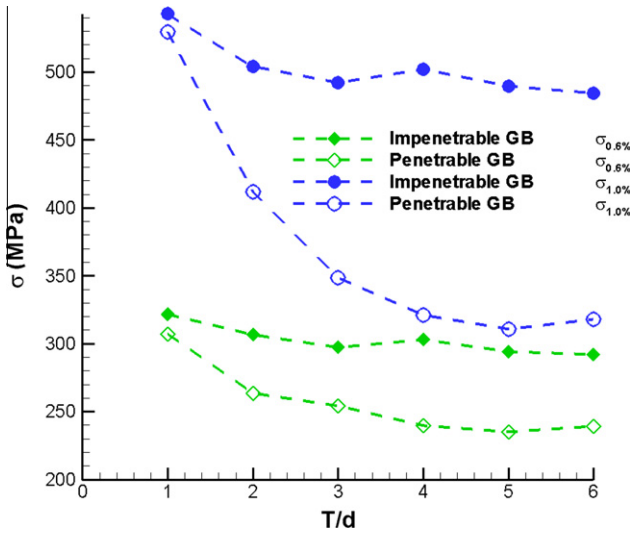

Fig. 12. Variations of the tensile strengths at different strains with T/d for passivated films with penetrable GBs and impenetrable GBs.

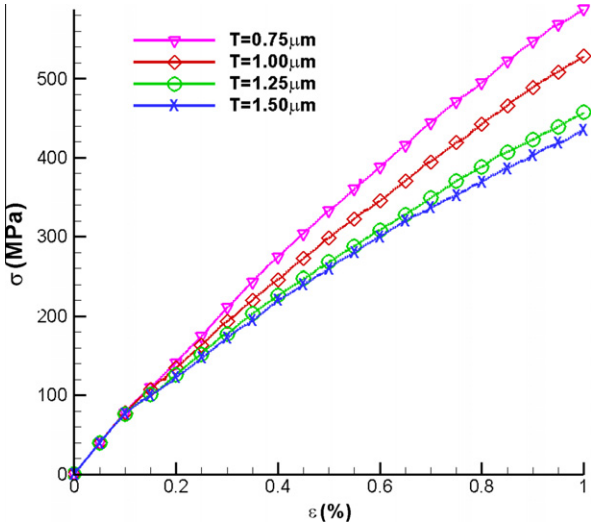

Fig. 13. Stress–strain response of the films with SGRZs with different thicknesses.

would prevail against that of the high stress region within SGRZs; as a result, the thickness effect would gradually vanish.

In fact, the competition between weakening and strengthening also exists in the films with SGRZs. The refined surface grains play a relative strengthening role in the overall tensile strength and the interior grains act a relative weakening part. With the increase of film thickness, the relative weakening within the interior region gradually exceeds the relative strengthening in the surface region, which is the same as the process of films with SPLs but opposite to that of films without surface treatment. According to this viewpoint of the competition between weakening and strengthening

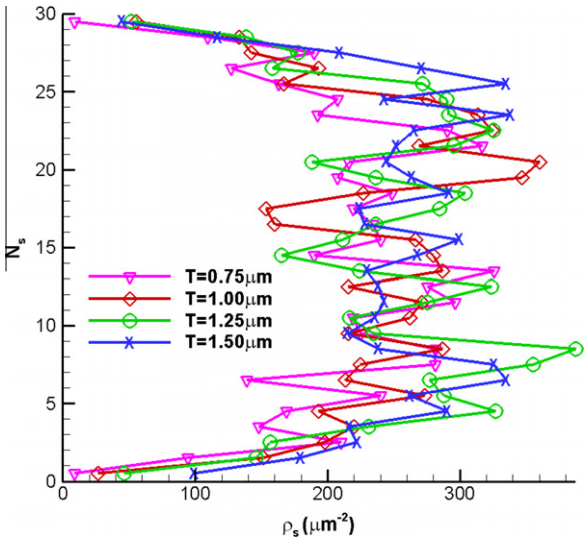

Fig. 14. Through-thickness distribution of ρ_s at $\varepsilon = 1.0\%$.

(actually the competition between exterior surface-constraint and interior GB-constraint), different thickness effects displayed in different kinds of thin films mainly depend on different spatial distributions of the weakening zone and strengthening zone in the thickness direction of films. If the exterior surface-constraint is weaker than the interior GB-constraint, such as in the films without surface treatment, the exterior free surface-constraint acts as weakening and the interior GB-constraint does as strengthening, so the thickness effect of "thicker is stronger" is displayed. Oppositely, in the films with SPLs and SGRZs, the exterior surface-constraints induced by SPLs and SGRZs are much stronger than the interior GB-constraints. The opposite spatial distributions of the strengthening zone and relative weakening zone in the thickness direction of thin films with surface treatments result in the opposite thickness effect of "thinner is stronger". No matter in what type of thin films, when the number of grains in the thickness direction is large enough, the interior GB-constraint would prevail against the exterior surface-constraint and thickness effects disappear.

4. Concluding remarks

Using the two-dimensional DDD framework which was proposed by Van der Giessen and Needleman (1995) and further extended by Li et al. (2009) with incorporation of the penetrable dislocation-GB interaction model, we studied the thickness effect on the tensile strength of polycrystalline thin films, with a special emphasis on the competition between the exterior surface-constraint and interior GB-constraint. Three kinds of polycrystalline thin films were considered, including the thin films (i) without

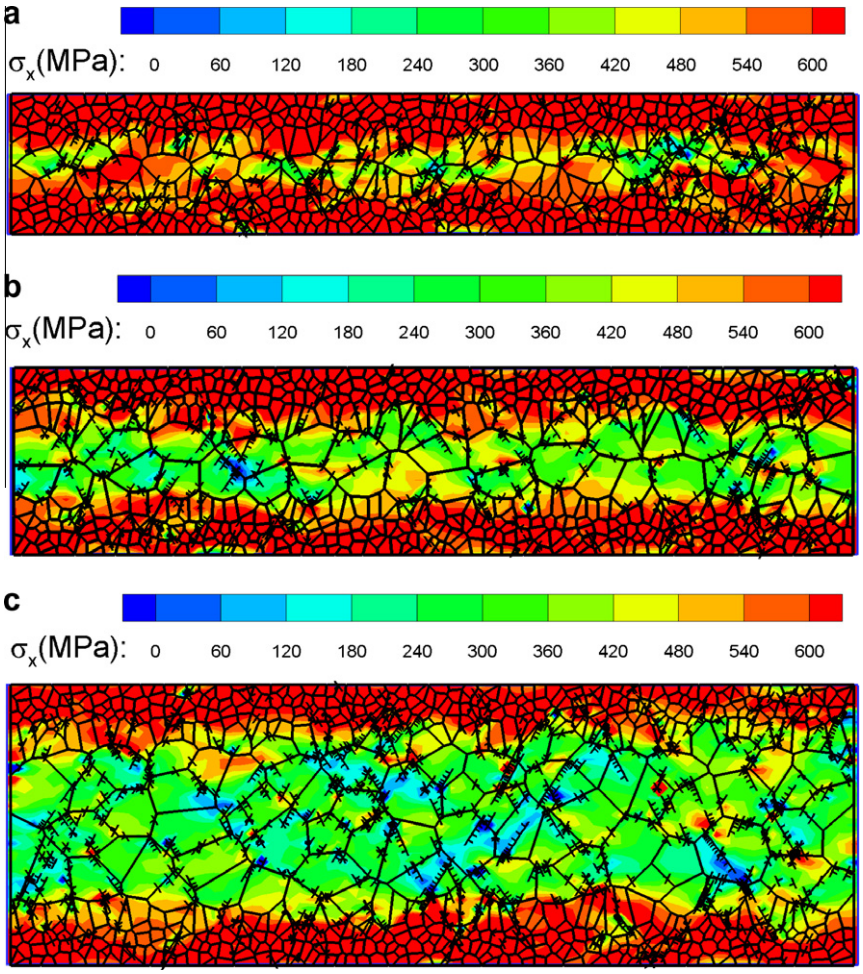

Fig. 15. Dislocation pattern and contour of tensile stress σ_x at $\varepsilon = 1.0\%$ in the films with different thicknesses: (a) $T = 0.75$ μm, (b) $T = 1.00$ μm and (c) $T = 1.50$ μm. The symbols "⊥" represent dislocations.

surface treatment, (ii) with SPLs and (iii) with SGRZs. From our computations, some conclusions can be drawn:

- In the thin films without surface treatment, there exists strong thickness effect on the overall tensile strength of thin films, i.e., thicker is stronger. The main reason inducing this thickness effect is the competition between the exterior surface-constraint and interior GB-constraint on gliding dislocations. As we know, the free surface-constraint on dislocations is much weaker than the interior GB-constraint even though the GBs are penetrable by dislocations. Consequently, the free surface-constraint induces weakening effect and the tensile stress in surface grains is low. On the contrary, the interior GB-constraint induces strengthening effect and the tensile stress in interior grains is high. When the number of grains in the thickness direction is small, i.e., 1 or 2, surface grains are in the majority and the weakening induced by free surface-constraint dominates the overall tensile strength. With the increase of the number of grains in the thickness direction, the percentage of interior grains in total grains increases, so the strengthening induced by interior GB-constraint makes an increasing contribution to the overall tensile strength, displaying the thickness effect of "thicker is stronger". When the number of grains in the thickness direction becomes large enough, the strengthening substantially prevails against the weakening and thus this thickness effect vanishes. In addition, the critical grain number in the thickness direction, above which no thickness effect occurs any more, is about 4 according to our computations.
- In the polycrystalline thin films with SPLs, the tensile strength displays the opposite thickness effect, i.e., thinner is stronger. The main reason behind this thickness effect is also the competition between the surface-constraint and interior constraint on gliding dislocations. Only the passivated surface-constraint plays a strengthening role while the interior GB-constraint does a relative weakening one, which is opposite to the thin films without surface treatment. Therefore, the opposite spatial distributions of the strengthening zone and the relative weakening zone in the thickness direction yields this opposite thickness effect.
- In the thin films with SGRZs, the thickness effect on the tensile strength is similar to that in the thin films with SPLs, i.e., thinner is stronger. However, the underlying dislocation mechanisms in those two cases are different. In the films with SPLs, the dislocation density within boundary layers near the film-passivation interfaces sharply increases due to the strong constraint of passivated surfaces. However, in the films with SGRZs, the dislocation density within the SGRZs sharply decreases because of the reduction of surface grain size to nanometer scale. As is well known, plastic strain mainly comes of the movements of dislocations. In the films with SPLs, the dislocations within boundary layers are difficult to glide and consequently the plastic strain is low there. On the other hand, in the films with SGRZs, dislocations are difficult to nucleate and glide within SGRZs and thus the plastic strain is also low there. As a result, the tensile stress within both the boundary layers and SGRZs is high. It is not difficult to understand that the passivated surface-constraint and refined surface grain constraint induce the same effect, i.e., the strengthening effect. Hence, with the increase of film thickness, the same spatial distributions of the hardening zone and the relative weakening zone in the thickness direction result in the same thickness effect, i.e., thinner is stronger.

It should be pointed out that, there are two characteristic sizes in polycrystalline thin films, i.e., grain size d and film thickness T. The effect of grain size d on the strength of polycrystalline films (i.e., Hall–Petch effect) originates from the constraint of GBs on dislocations and the effect of film thickness T (i.e., thickness effect) mainly arises from the competition between the interior GB-constraint and exterior surface-constraint. In this contribution, only the thickness effect is paid a special attention to but the grain size effect is ignored by keeping d unchanged. In addition, only two-dimensional plane strain discrete dislocation dynamics method is employed in this paper for simplicity. Although some important three-dimensional dislocation mechanisms are ignored, some interesting results in good agreement with the existing experiments can still be captured by present computations. These results are helpful for us to understand the thickness effect on the tensile strength of polycrystalline thin films and the associated dislocation mechanisms.

Acknowledgments

The authors want to express their thanks for the financial support from NSFC under the Grant Number 10672064. In addition, the pertinent comments from anonymous reviewers are helpful to improve this paper.

References

Akarapu, S., Zbib, H.M., Bahr, D.F., 2010. Analysis of heterogeneous deformation and dislocation dynamics in single crystal micropillars under compression. Int. J. Plasticity 26, 239–257.

Arzt, E., 1998. Size effects in materials due to microstructural and dimensional constraints: a comparative review. Acta Mater. 46, 5611–5626.

Balint, D.S., Deshpande, V.S., Needleman, A., Van der Giessen, E., 2008. Discrete dislocation plasticity analysis of the grain size dependence of the flow strength of polycrystals. Int. J. Plasticity 24, 2149–2172.

Bayley, C.J., Brekelmans, W.A.M., Geers, M.G.D., 2007. A three-dimensional dislocation field crystal plasticity approach applied to miniaturized structures. Philos. Mag. 87, 1361–1378.

Cleveringa, H.H.M., Van der Giessen, E., Needleman, A., 1999. A discrete dislocation analysis of bending. Int. J. Plasticity 15, 837–868.

Deshpande, V.S., Needleman, A., Van der Giessen, E., 2005. Plasticity size effects in tension and compression of single crystals. J. Mech. Phys. Solids 53, 2661–2691.

Espinosa, H.D., Panico, M., Berbenni, S., Schwarz, K.W., 2006. Discrete dislocation dynamics simulations to interpret plasticity size and surface effects in freestanding FCC thin films. Int. J. Plasticity 22, 2091–2117.

Espinosa, H.D., Prorok, B.C., Peng, B., 2004. Plasticity size effects in free-standing submicron polycrystalline FCC films subjected to pure tension. J. Mech. Phys. Solids 52, 667–689.

Geers, M.G.D., Brekelmans, W.A.M., Bayley, C.J., 2007. Second-order crystal plasticity: internal stress effects and cyclic loading. Model. Simul. Mater. Sci. Eng. 15, 133–145.

Geers, M.G.D., Brekelmans, W.A.M., Janssen, P.J.M., 2006. Size effects in miniaturized polycrystalline FCC samples: strengthening versus weakening. Int. J. Solids Struct. 43, 7304–7321.

Guruprasad, P.J., Benzerga, A.A., 2008. Size effects under homogeneous deformation of single crystals: a discrete dislocation analysis. J. Mech. Phys. Solids 56, 132–156.

Hasson, G.C., Goux, C., 1971. Interfacial energies of tilt boundaries in aluminium. Experimental and theoretical determination. Scr. Metall. 5, 889–894.

Hou, C., Li, Z., Huang, M., Ouyang, C., 2009. Cyclic hardening behavior of polycrystals with penetrable grain boundaries: two-dimensional discrete dislocation dynamics simulation. Acta Mech. Solida Sin. 22, 295–306.

Hull, D., Bacon, D.J., 2001. Introduction to Dislocations, fourth ed. Butterworth–Heinemann.

Keller, C., Hug, E., Feaugas, X., 2011. Microstructural size effects on mechanical properties of high purity nickel. Int. J. Plast. 27, 635–654.

Kubin, L.P., Canova, G., Condat, M., Devincre, B., Pontikis, V., Brechet, Y., 1992. Dislocation microstructures and plastic flow: a 3D simulation. Solid State Phenom. 23–24, 455–472.

Kumar, R., Nicola, L., Van der Giessen, E., 2009. Density of grain boundaries and plasticity size effects: a discrete dislocation dynamics study. Mater. Sci. Eng. A 527, 7–15.

Kumar, R., Szekely, F., Van der Giessen, E., 2010. Modelling dislocation transmission across tilt grain boundaries in 2D. Comput. Mater. Sci. 49, 46–54.

Lee, S.-W., Aubry, S., Nix, W.D., Cai, W., 2011. Dislocation junctions and jogs in a free-standing FCC thin film. Model. Simul. Mater. Sci. Eng. 19, 025002.

Li, Z., Hou, C., Huang, M., Ouyang, C., 2009. Strengthening mechanism in micro-polycrystals with penetrable grain boundaries by discrete dislocation dynamics simulation and Hall–Petch effect. Comput. Mater. Sci. 46, 1124–1134.

Liang, X., Wang, B., Liu, Y., 2009. Thickness effect of a thin film on the stress field due to the eigenstrain of an ellipsoidal inclusion. Int. J. Solids Struct. 46, 322–330.

Miyazaki, S., Shibata, K., Fujita, H., 1979. Effect of specimen thickness on mechanical properties of polycrystalline aggregates with various grain sizes. Acta Metall. 27, 855–862.

Nicola, L., Van der Giessen, E., Needleman, A., 2003. Discrete dislocation analysis of size effects in thin films. J. Appl. Phys. 93, 5920–5928.

Nicola, L., Van der Giessen, E., Needleman, A., 2005a. Size effects in polycrystalline thin films analyzed by discrete dislocation plasticity. Thin Solid Films 479, 329–338.

Nicola, L., Van der Giessen, E., Needleman, A., 2005b. Two hardening mechanisms in single crystal thin films studied by discrete dislocation plasticity. Philos. Mag. 85, 1507–1518.

Nicola, L., Xiang, Y., Vlassak, J.J., Van der Giessen, E., Needleman, A., 2006. Plastic deformation of freestanding thin films: experiments and modeling. J. Mech. Phys. Solids 54, 2089–2110.

Ouyang, C., Li, Z., Huang, M., Fan, H., 2010. Cylindrical nano-indentation on metal film/elastic substrate system with discrete dislocation plasticity analysis: a simple model for nano-indentation size effect. Int. J. Solids Struct. 47, 3103–3114.

Ouyang, C., Li, Z., Huang, M., Hou, C., 2008. Discrete dislocation analyses of circular nanoindentation and its size dependence in polycrystals. Acta Mater. 56, 2706–2717.

Raulea, L.V., Goijaerts, A.M., Govaert, L.E., Baaijens, F.P.T., 2001. Size effects in the processing of thin metal sheets. J. Mater. Process. Technol. 115, 44–48.

Shen, Z., Wagoner, R.H., Clark, W.A.T., 1986. Dislocation pile-up and grain boundary interactions in 304 stainless steel. Scr. Metall. 20, 921–926.

Shen, Z., Wagoner, R.H., Clark, W.A.T., 1988. Dislocation and grain boundary interactions in metals. Acta Metall. 36, 3231–3242.

Shishvan, S.S., Mohammadi, S., Rahimian, M., Van der Giessen, E., 2011. Plane-strain discrete dislocation plasticity incorporating anisotropic elasticity. Int. J. Solids Struct. 48, 374–387.

Tang, H., Schwarz, K.W., Espinosa, H.D., 2007. Dislocation escape-related size effects in single-crystal micropillars under uniaxial compression. Acta Mater. 55, 1607–1616.

Tsai, M.C., Chen, Y.A., Wu, C.F., Chen, F.K., 2005. Size-effects in micro-metal sheet forming of unalloyed copper and brass. Adv. Mater. Res. 6–8, 705–712.

Van der Giessen, E., Needleman, A., 1995. Discrete dislocation plasticity: a simple planar model. Model. Simul. Mater. Sci. Eng. 3, 689–735.

Xiang, Y., Tsui, T.Y., Vlassak, J.J., 2006. The mechanical properties of freestanding electroplated Cu thin films. J. Mater. Res. 21, 1607–1618.

Xiang, Y., Vlassak, J.J., 2006. Bauschinger and size effects in thin-film plasticity. Acta Mater. 54, 5449–5460.